Present and future trends in excimer laser based microlithography

Frank K. Tittel, M. Erdelyi, Z.L. Horvath+, Armen Kroyan, William Wilson, Michael Smayling*, Zs. Bor+, and G. Szabo+
Department of Electrical & Computer Engineering, Rice University
P.O. Box 1892, Houston, Texas 77251-1892
*Texas Instruments, Inc., 12201 S.W. Freeway, Stafford, Texas 77477
+Department of Optics & Quantum Electronics, JATE University, H6720 Szeged, Hungary

ABSTRACT

Optical microlithography is continuing to play a key role in the fabrication of feature sizes in the 0.25-0.1 μm regime as the semiconductor industry enters manufacturing of the gigabit chip generation. Several important advances in technologies are needed to achieve this goal. These include the use of excimer lasers and optical resolution enhancement schemes, which will be addressed in this work.

1. INTRODUCTION

Optical microlithography is the key technology that has driven the dynamic growth of the microelectronics industry over the past two decades.[1-3] Deep-UV lithography using 248 and 193 nm light will be the microlithography technology of choice for the fabrication of advanced memory and logic devices for the next decade. The next generation of microprocessors and 256 Mbit DRAM memory chips will require minimum feature sizes of 0.25 micron. Both the Moore curve and the U.S. Semiconductor Industry Association (SIA) road map[1] provide a means of projecting future trends for integrated circuit technology (Fig. 1). Resolution (W_{min}) and depth of focus (DOF) in microlithography are limited by diffraction as the light is

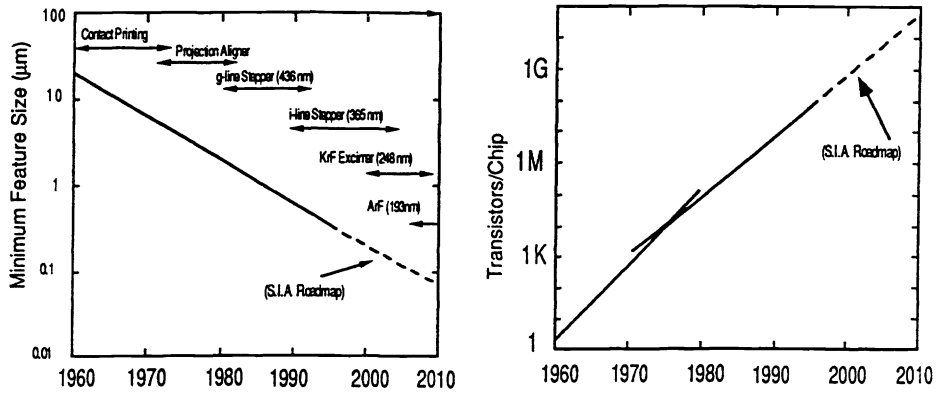

Fig. 1: SIA road map for minimum feature size and number of transistors per chip from 1960 to 2010.

transmitted by the mask or reticle and projected on to a photoresist coated silicon wafer. The lithography equations are given by:

$$W_{min} = k_1 \frac{\lambda}{NA}$$
$$DOF = k_2 \frac{\lambda}{NA^2} \quad (1)$$

where NA is the numerical aperture of the projection lens and assuming that the degradation of resolution results entirely from diffraction. One can improve resolution and DOF by resorting to shorter wavelengths (λ), high numerical aperture lenses, and optical enhancement methodologies by manipulating the k_1 and k_2 factors (as depicted in Fig. 2) in state of the art optical steppers. Hence it should be possible to process wafers with 130 nm features using 193 nm excimer laser lithography. The challenge that we have started to address is to develop an optical enhancement scheme that can be readily introduced in a commercial excimer laser based optical stepper as the semiconductor industry is transitioning to the introduction of 256 Mbit

and 1 Gbit dynamic random access memory (DRAM's). Beyond 130 nm, integrated circuit devices may require soft x-rays[4], electron or ion beams. KrF and ArF excimer lasers operating at 248 nm and 193 nm are particularly suited for sub-quarter micron microlithography. Specific merits include: natural narrow spectral bandwidth, on command illumination, constant and efficient power output, precise dose control, more energy at the wafer plane illumination, ideally suited for annular and quadrupole illumination. Size and initial cost compared to a Hg lamp illumination system may be considered a shortcoming.

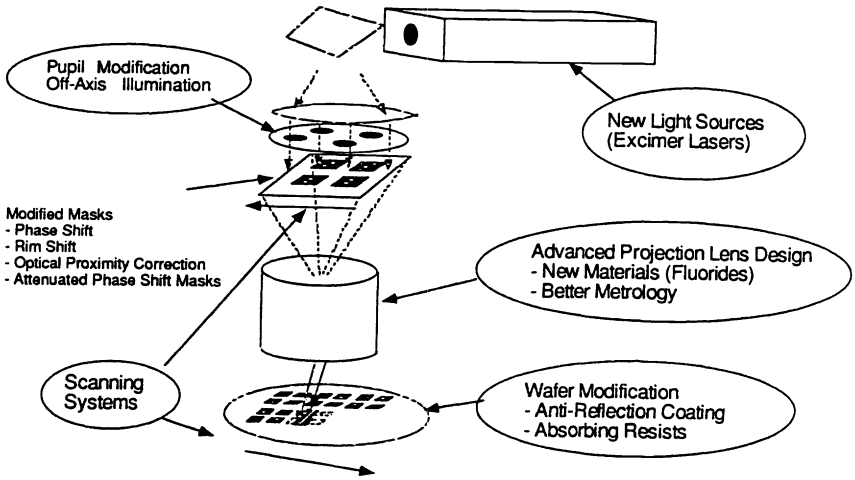

Fig. 2: Optical enhancement schemes for use in optical steppers.

2. GENERATION OF DIFFRACTION-FREE BEAMS

In 1987 Durnin[5] showed that the field described by

$$E(r,z,t) = A \cdot J_0(k_\perp r) \cdot e^{i(k_\parallel z - \omega t)} \tag{2}$$

is an exact solution of the wave equation

$$\left(\nabla^2 - \frac{1}{c^2}\frac{\partial^2}{\partial t^2}\right) E(r,z,t) = 0. \tag{3}$$

where $k_\perp^2 + k_\parallel^2 = \omega^2 / c^2$, and J_0 is the zero-order Bessel function of the first kind. This field represents a nondiffracting beam because the transverse intensity distribution is independent of the propagation distance z. Such an ideal beam cannot be realized experimentally over large values of z and r, because the electric-field amplitude of the beam cannot be spatially integrated and would be exact only in infinite free space.[5,6]

This paper reports an experimental demonstration of a technique which is capable of enhancing the transverse resolution and depth of focus (DOF) in optical microlithography using nearly nondiffracting Bessel beams generated with a Fabry-Perot etalon. This technique can be a useful procedure in the fabrication of various integrated circuit feature geometries, because it significantly enhances the transverse resolution and simultaneously increases the depth of focus. Since in optical microlithography 1-2 μm DOF is sufficient, our purpose (in contrast with Refs. 5,6) is not to generate large-range constant-axial-intensity beams, but increase the DOF only by a factor of about 2. In our experiments[7] the Fabry-Perot etalon is placed after the reticle and directly in front of the projection lens, and there is no other lens between the etalon and projection lens.

3. EXPERIMENTAL DESCRIPTION

The experimental arrangement is depicted in Figure 3. A He-Ne laser operating at 632.8 nm illuminates a microscope objective (NA = 0.65). Due to the relatively high numerical aperture, the objective creates a nearly point-like light source.

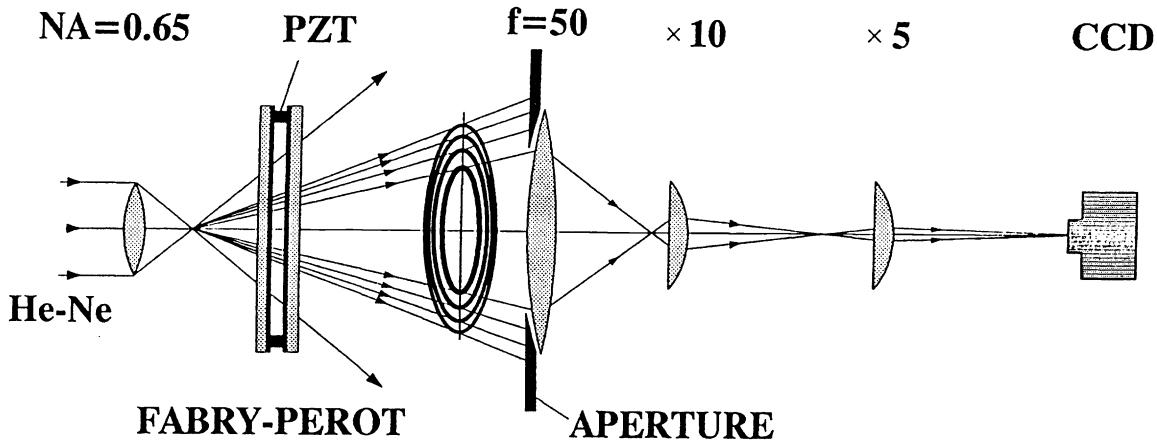

Fig. 3: Schematic diagram of the experimental setup. The aperture of the objective lens transmits the first Fabry-Perot ring and blocks all other rings. The image is magnified by means of two microscope objectives and observed with a CCD camera.

This point source illuminates a scanning Fabry-Perot etalon (Tropel CL-100) which produces a concentric ring system behind the etalon. The aperture of an objective lens placed after the interferometer is adjusted to that it transmits only the first Fabry-Perot ring (at the rim of the aperture) and blocks all the others. Due to multiple reflections in the interferometer (see Figure 4), the real point-like source I_0 creates several virtual images (I_1, I_2, I_3, ...). The distance between these images is

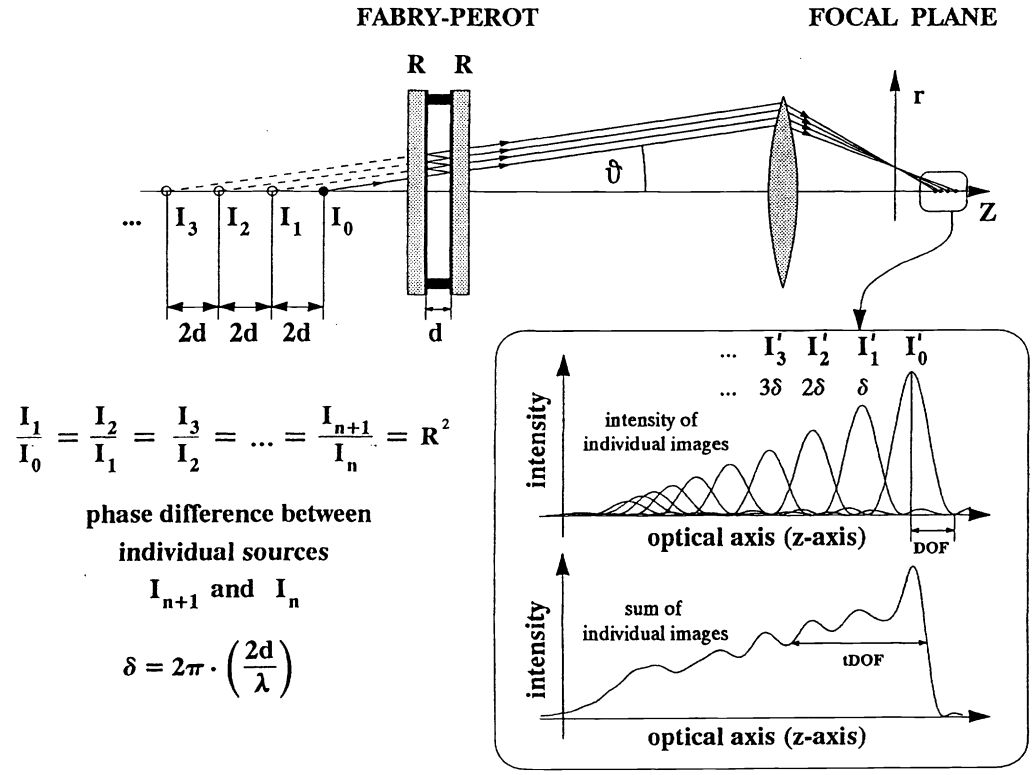

Fig. 4: The image produced by the objective lens is the superposition of the images (I'_0, I'_1, I'_2, ...) of the individual point sources. Therefore, N (relative image density) is an important factor[7] in determining the shape of the axial intensity distribution.

2d (d is the separation of the etalon mirrors), and the intensity ratio is R^2 between adjacent individual sources, where R is the reflectivity of the Fabry-Perot mirrors. The measured value of R is 96.2%. The distance between the virtual point sources can be changed easily as the separation of the etalon mirror is adjustable with a piezo translator. The relative phase difference (δ) between the adjacent point sources is related to d by

$$\delta = 2\pi \cdot \frac{2d}{\lambda} . \tag{4}$$

The image produced by the objective is the superposition of the images of individual point sources. The distance between these points is $2dM^2$, where M^2 is the longitudinal magnification of the objective lens. The image produced by the objective lens is magnified by two microscope objectives in tandem (with about 100 overall magnification) and monitored with a CCD camera (COHU 4810, horizontal center-to-center spacing of pixels: 23 μm). The first microscope objective is mounted on a precision translator, and thus the axial intensity distribution could also be examined.

It should be noted that this technique is similar to the FLEX method[8] where several focal planes are created at different positions along the optical axis, and exposures are made at each focal plane. Our technique based on nondiffracting Bessel beams creates multiple images of the mask onto the wafer but requires no mechanical translational shift.

The theoretically predicted intensity distribution in planes perpendicular to the optical axis is a J_0 function.[9] The measured intensity distribution supports this prediction (see Figure 5). The circles depict the measured intensity distribution, and the solid line shows the fitted J_0 Bessel function. A comparison of the measured Bessel distribution and the Airy pattern shows (with good agreement of the theoretical description) that the FWHM of the Bessel beam is 1.6 times smaller than the FWHM of the Airy pattern. This decrease means an enhancement in the transverse resolution power.

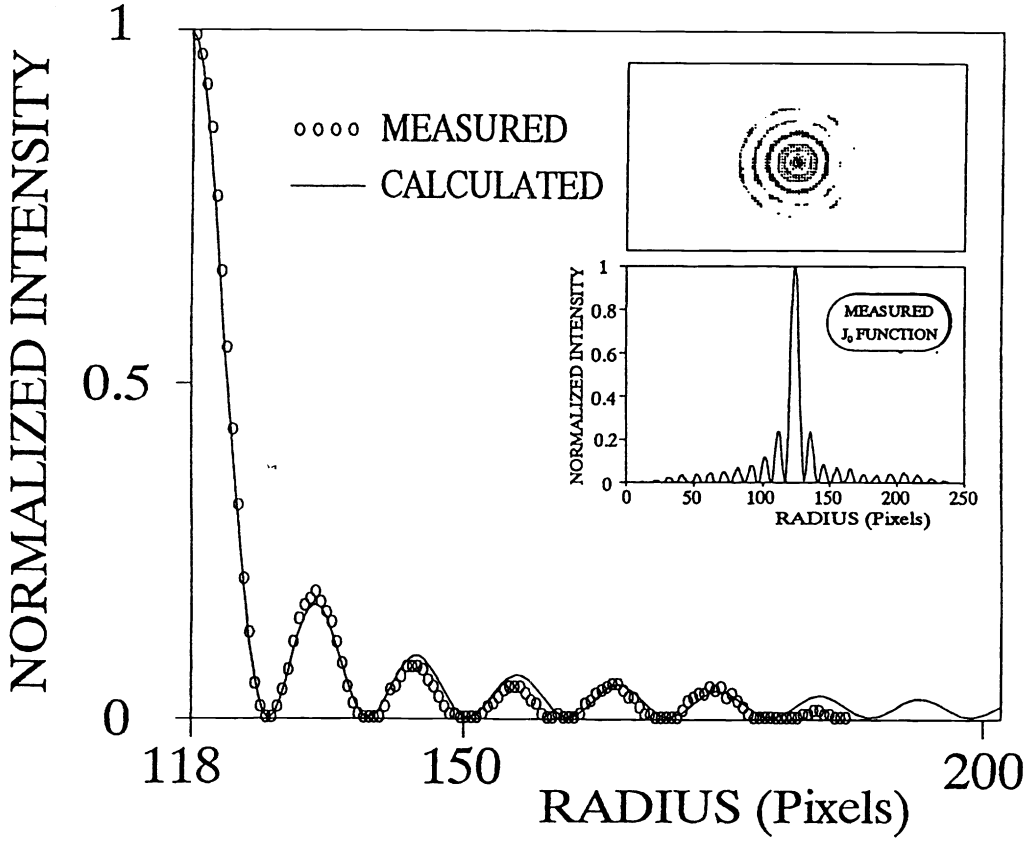

Fig. 5: The measured intensity distribution perpendicular to the optical axis is quasi-equivalent to a zero order Bessel function. The solid line shows the fitted curve to the measured intensity distribution (depicted by circles).

4. THEORETICAL DESCRIPTION BASED ON THE SOLUTION OF DIFFRACTION INTEGRAL

In addition to the experimental study, the spatial intensity distribution was calculated numerically using a wave optics model. The total electric field behind the projection lens is the superposition of the fields of the individual sources:[9]

$$E(r,z) = -\frac{ikA_0}{2} \cdot \exp[i(kz + \Phi_0)] \cdot \sum_{m=0}^{\infty} \frac{[R \cdot \exp(i\delta)]^m}{p_m q_m} (C(u_m, v_m) - iS(u_m, v_m)) \,, \tag{5}$$

where k is the wave number; A_0 is the amplitude of the first (real) source; Φ_0 is a phase factor; R is the reflectivity of the mirrors; δ is the phase shift introduced by the Fabry-Perot interferometer; p_m, q_m are the radius of the incoming and outgoing spherical waves; u, v are dimensionless variables; $C(u_m,v_m)$ and $S(u_m,v_m)$ functions can be calculated by the Lommel functions. Figure 6 depicts the results of the calculations. The insets show the comparison of the measured (dotted line) and the calculated (solid line) intensity distribution on the optical axis. In the first case (when the relative image density N, defined as the ratio of DOF and distance between image points beyond the projection lens, equals 0.5), the distance between the image points is twice the DOF; therefore, the images can be observed separately. By decreasing the distance between the image points, the sharp peaks disappear and the intensity decreases faster on the optical axis. From the microlithographic point of view, oscillations in the intensity distribution are undesirable. By increasing the N ratio, the curves become smoother and the oscillations disappear. In the last case (N=10), no oscillations occur. Since, in case of superimposed images, the first minimum is not zero, it is necessary to give a new definition of DOF, so called tDOF. tDOF is defined as the range where the intensity is higher than 50% of the main peak. The figures show normalized intensity, but in reality (due to the law of conservation of energy) by increasing the N ratio, the intensity of the main peak increases. The N=4 case appears to be the optimum for microlithographic applications. The oscillations are absent, and the tDOF range is twice as large as without the Fabry-Perot etalon.

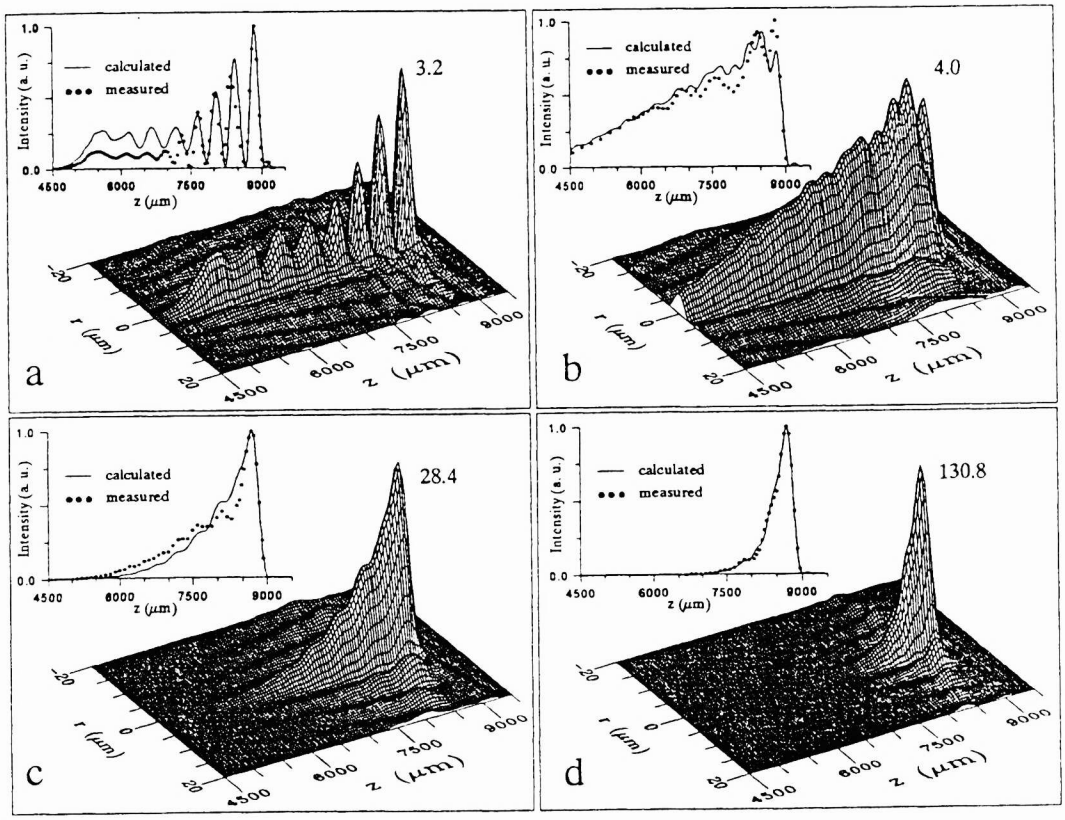

Fig. 6: The spatial intensity distribution as calculated from Eq. (5) for different values of image density N and reduced phase difference δ_r.[9] The insets show a comparison of the measured and calculated axial intensity distribution. The numbers adjacent to the peaks display the intensity maxima in arbitrary units.

5. DISCUSSIONS AND CONCLUSIONS

In summary, wavefront engineering applied to excimer laser based exposure tools (optical steppers) coupled to 300 mm diameter silicon wafers will allow optical microlithography to be used well into the first two decades of the next century with the fabrication of complementary metal oxide semoconductor (CMOS) devices requiring minimum feature sizes at or less than 130 nm. A novel concept for resolution and DOF enhancement in optical microlithography based on generating a diffraction-free beam with a Fabry-Perot etalon has been proposed. Preliminary experimental results in the visible have shown that this technique significantly increases both the DOF and the transverse resolution. This technique is especially effective when applied to small isolated patterns like contact holes. It was shown that even in the most critical case, undesirable interference effects between adjacent contact holes can be eliminated by means of a phase shifting mask. For more complex geometries (line/spaces, elbows, etc.) and KrF excimer laser illumination, the applicability of this technique needs further investigation. Such parameters as separation, reflectivity, and insertion point of the Fabry-Perot etalon have to be considered for use of this approach in an optical stepper.

6. ACKNOWLEDGMENTS

This research was supported in part by Texas Instruments, Inc., and the Hungarian Academy of Sciences Foundation (OTKA).

7. REFERENCES

1. P. Rai-Choudhury (ed.), *Handbook of Microlithography, Micromachining and Microfabrication, Vol. 1: Microlithography,* SPIE Optical Engineering Press (1997).
2. K. Jain, *Excimer Laser Lithography*, SPIE Optical Engineering Press (1990).
3. G. Zorpette, "The Solid-State Century," Special Issue, Vol. 8, *Scientific American* (1997).
4. A.M. Hawryluk, N.M. Ceglio, and D.A. Merkle, "EUV Lithography," *Microlithography World* 6, 17 (Summer 1997).
5. J. Durnin, J.J. Miceli, Jr., and J.H. Eberly, "Diffraction-Free Beams," *Phys. Rev. Lett.* 58, 1499 (1987).
6. A.J. Cox and D.C. Dibble, "Nondiffracting Beams from a Spatially Filtered Fabry-Perot Resonator," *J. Opt. Soc. Am.* 2, 282 (1992).
7. M. Erdélyi, Z.L. Horváth, G. Szabó, Zs. Bor, F.K. Tittel, J.R. Cavallaro, and M.C. Smayling, "Generation of diffraction-free beams for applications in optical microlithography," *J. Vac. Sci. Technol. B* 15, 287 (1997).
8. Hiroshi Fukuda, Norio Hasegawa, and Shinji Okazaki, "Improvement of defocus tolerance in a half-micron optical lithography by the focus latitude enhancement exposure method: Simulation and experiment," *J. Vac. Sci. Technol. B* 7, 667-674 (1989).
9. Z.L. Horváth, M. Erdélyi, G. Szabó, Zs. Bor, F.K. Tittel, and J.R. Cavallaro, "Generation of nearly nondiffracting Bessel beams with a Fabry-Perot interferometer," *J.Opt. Soc. Am. A* 14, 3009 (1997).